Taylor & Francis
Taylor & Francis Group

Journal of Building Performance Simulation

ISSN: (Print) (Online) Journal homepage: https://www.tandfonline.com/loi/tbps20

Achieving realtime daylight factor computation for modular buildings in generative design

Xavier Marsault

To cite this article: Xavier Marsault (2022) Achieving realtime daylight factor computation for modular buildings in generative design, Journal of Building Performance Simulation, 15:6, 848-865, DOI: 10.1080/19401493.2022.2102676

To link to this article: https://doi.org/10.1080/19401493.2022.2102676

Published online: 04 Aug 2022.

JOURNAL OF BUILDING PERFORMANCE SIMULATION
2022, VOL. 15, NO. 6, 848–865
https://doi.org/10.1080/19401493.2022.2102676

Achieving realtime daylight factor computation for modular buildings in generative design

Xavier Marsault

UMR CNRS MAP 3495; National School of Architecture, Lyon University, Lyon, France

ABSTRACT

In generative design, it is imperative for an architect to evaluate very quickly the performance of many buildings produced. Knowing in interactive time the daylighting potential of a generated form at an early stage of its design, with a minimum of parameters, allows to quickly choose among many variants. The daylight factor computational metamodel presented here in the case of modular buildings allows to instantly compare these solutions in order to make judicious choices in dimensioning, without performing time-consuming simulations. Another challenge was to achieve realtime computation for the daylight factor without using a GPU. We have addressed this objective via an hybrid computation both based on physical and statistical modeling, and on a physical-based computation engine specifically used for the optimization of buildings composed of multiple living units. We detail the full implementation in a generative design software leading to impressive computation times of the order of one ms.

ARTICLE HISTORY
Received 22 July 2021
Accepted 8 July 2022

KEYWORDS
Daylight factor; realtime computation; hybrid metamodel; voxel-based building; generative design

1. Introduction

1.1. Objectives of this research

The average daylight factor (*DF*) on a work surface is recognized as a good indicator of the luminous performance of a room, especially during the design phase. In that context, the objective of our research was to build a simplified but sufficiently accurate model for the very fast calculation of the daylight factor of one or more modular buildings composed of many rooms, designed on the basis of voxels (section 1.2), in a partially occulted urban area. In such a complex scene, as noticed in (Cheung and Chung 2005; Mavromatidis, Marsault, and Lequay 2014; Li et al. 2017), there are many objects more or less close, occulting the light at an opening of a façade: natural ground, ground with slope, embankments, buildings, urban furniture, trees and massifs, without forgetting some facades of the building itself (self-shading).

Even if some recent papers succeed in accelerating *DF* computation (reaching to 2-order-of-magnitude speed), by means of GPU-based methods, currently there remains a gap in obtaining realtime accurate global illumination results for building designers in real time (3-order-of-magnitude speed) for arbitrary building shapes (section 2.3). Of course, as GPUs become more and more powerful, especially since the release of Nvidia RTX cards dedicated to ray tracing, physics-based simulations are progressing inexorably towards real time.

Performance computation generally refers to physics models that can be implemented and simplified enough in order to attain fast speed with the aid of multicore CPUs and GPUs. Performance metamodels rather refer to statistical approaches that can be considered for assessment as shorcuts or black-boxes. In our present research, we have called upon both physics and metamodels, without the use of any expensive hardware like powerfull GPUs. Our paper shows that, sometimes, it is possible to go beyond the possibilities of current GPUs with multicore CPUs for some massive light performance calculations, especially usefull in generative design. We present the whole approach for the specific case of multi-storey modular buildings whose morphology will be described.

Voxel-based computation has been widely used during the last decades in the field of Building Simulation (BS), and is still efficient in the early stages of many project designs. Despite its raw geometric nature, it remains often used for the sake of simplicity and performance, and commonly implemented to simplify the problem of optimizing morphological figures and the associated light calculations (Mavromatidis, Marsault, and Lequay 2014; Darmon 2018; Marsault and Torres 2019; Nault 2016; Jones and Reinhart 2015; Marsh and Stravoravdis 2017; De Luca

CONTACT Xavier Marsault xavier.marsault@aria.archi.fr UMR CNRS MAP 3495; National School of Architecture, Lyon University, Lyon, France

et al. 2019; Peters et al. 2019; Walger da Fonseca and Ruttkay Pereira 2021; Lin and Tsay 2021; Nourkojouri et al. 2021) in architecture and building simulation researches, in the early stages of a project, within an already built environment. Here, the fundamental volumes are easily distributed on a spatial grid contained in the total volume available for the installation of specific functions (e.g. housing, commercial, office, …), which makes it easier to precalculate illumination on surfaces.

We have first chosen to revisit and enrich a previous and efficient metamodel published in (Mavromatidis, Marsault, and Lequay 2014) for the *DF* assessment of voxels. Its calculation took into account the annual diffuse fluxes on a given site and simplified masks present in the field of view of the openings, which it converts into simplified masks for realtime queries. Certainly, this work was a pionner research few years ago, but it was not scalable for the voxel dimensions (great limitation), as explained in section 2.2.3. We then decided to use hybrid modeling (between physical and metamodelization) to solve the lack of this important feature: this is our first important contribution in this paper (section 3).

Moreover, implementing and using our new *DF* model within a generative design framework revealed the pertinence of our approach, that led to very light computations and opened the way to realtime assessements, particularly tested and appreciated in the architectural competition phase (second contibution, see section 4).

1.2. On the use of voxels in architecture

Cubic (or cuboidal) architecture has often inspired many architects. This was the case of Moshe Safdie who, in the 1960s, designed Habitat 67, a group of collective housing units located in Montreal and intended for the Expo 67 world fair. He was interested in high-density urban architecture and sought to reduce costs through the use of prefabricated modular elements of 11.7 m x 5.3 m x 3 m. In total, 354 modules were built on top of each other to form 148 apartments (Safdie 1961). A similar concept, that of incremental architecture in areas of shortage, was also built on a form of appropriation of modularity, with Weston Williamson's *Palestinian housing*project. Still with the idea of simplification, Granadeiro used a grammar of parallelepiped shapes to generate architectones (in the sense of Kasimir Malevich, founding artist of Suprematism), and developed a method to help design the geometric shape of a building considering its influence on energy performance (Granadeiro et al. 2013). The definition of form is a recurrent problem, which mainly raises the issue of creating shape grammars that conform to the needs of designers (Garcia 2017). Mainly for economic reasons, but also for computation simplifications, the architectural design of complicated shapes often uses simple elementary volumes or surfaces. This approach makes sense in the early stages of residential building design. These shapes are generally easier to construct than rounded or streamlined shapes and are therefore less expensive to build. These basic volumes are also consistent with the physical performance analysis performed in the early stages of design: solar gain, building compactness, etc. These basic building shapes will then be refined to a more detailed and realistic form. Many building systems based on this principle have emerged.

We can thus see that the use of parallelepipedic or related shapes can be a promising concept at the heart of the architecture itself, making it possible to simplify the initial design of one or more buildings while maintaining a representative level of detail for generating, parameterizing, and optimizing the modular geometry. For example, the Sylvania concept of Aquitanis, based on prefabricated modular wood-frame housing, aimed at developing small multi-family buildings (2–20 units). The buildings were broken down into functional modules of 3.5 m x 3.5 m, defining a basic layout according to the user's needs. Another example is Moovabat, a technological building, a living complex, energy efficient and versatile (The MOOVABAT project 2017). A final example is the VoxEL project (Bollinger, Grohmann, and Tessmann 2010), which was developed as part of a competition for a school of architecture in Stuttgart in collaboration with the Laboratory for Visionary Architecture. Modular design was the focus of their work and the advantages of an elementary unit in cube form were presented. The cubic module becomes the main component applied to a multitude of materials (wood, metal, cement, plastic), to all the components of the building (roof, load-bearing walls, floors, linings, openings, stairs, etc.) and declined for all the constructive systems (wood frame, metal, masonry structure, etc.). More recently, a generative application based on voxels and composition rules inspired by cellular automata has been released for the design of solar envelopes and optimized shapes in the context of district planning (Darmon 2018).

2. Previous work

2.1. Daylight metrics and building

Daylighting has long been recognized as a key factor in the design of energy-efficient buildings. However, illuminance, which corresponds to the human perception of how a surface is lit, is the only directly measurable photometric quantity (luminous flux received per unit area).

In the residential and tertiary sectors where we spend a lot of time, daylighting problems mainly respond to the growing needs for well-being, luminous and thermal comfort of occupants, as well as the provision of natural light for work. Daylight optimization at an early stage of design also refers to a way of designing architectural forms that take advantage of the prevailing urban context subject to the influence of existing shadow masks. The goal is to create a comfortable indoor environment while minimizing reliance on artificial lighting systems and electrical energy consumption, which can be as high as 30% according to the ICEB.

Access to natural light is therefore not simply a technical or economic constraint, but also a source of well-being (winter and summer) and a factor in health and productivity. In this field, we are generally interested in three types of objectives that we hope to be able to achieve together: the ability of a building to let natural light into its interior spaces, its autonomy in natural lighting, and the characterization of its summer comfort (often by estimating the number of hours of discomfort). Dealing with the design of a building's natural lighting in the architectural sketch phase, during a programme or a construction competition, can then lead to innovations for architects, engineers and project management teams, particularly in terms of eco-responsible solutions.

Over the past twenty years, the main research has focused on:

- a) the availability of natural light, often interpreted by the value of the daylight factor which is expressed as a percentage (Cheung and Chung 2005; Li et al. 2017). This measure is defined as the ratio between the indoor illuminance received at a point on a reference plane (often a working plane or floor) and the outdoor illuminance available simultaneously on a horizontal plane in a perfectly clear site. The *DF* takes into account the size and layout of the room, the size and position of the windows, external obstructions, the reflectance of materials, and the transparency of glazing. Direct sunlight is excluded from this calculation, which is based solely on the light input from an overcast sky. Until recently, the *DF* has been the basis for many building standards and design guidelines for daylighting and visual ergonomics (French NF EN 12464–1 and NF X 35-103, European Daylight Standard EN-17037). It has been used to make rapid comparisons of daylight penetration in living spaces under overcast conditions, although its use is less justified in very sunny areas of the world (De Luca et al. 2019).

In 2003, the International Commission on Illumination (CIE) adopted a range of fifteen standardized skies covering the entire spectrum of clear and obscured skies (Perez, Seals, and Michalsky 1993) (ISO 15469:2004(E) and CIE S 011/E:2003). The best known models for calculating sky luminance are the Perez sky (Perez, Seals, and Michalsky 1993), the Igawa model (Igawa et al. 2004), and the CIE standard overcast model (CIE. "Natural daylight' 1955; Nabil and Mardaljevic 2006). The *DF* appears here as a dimensionless quantity depending only on the volume under test and its own characteristics. The indoor illuminance at a point is the sum of three components: the light emitted directly from the sky, the light reflected from the outdoor environment and the light reflected from the indoor surfaces (walls, floor, ceiling). The sky component has by far the greatest influence on the final result. Thus, the degree of sky obstruction is of paramount importance to the level of daylight reaching a window, and thus the interior of the room. Many papers have studied the approach to calculate the *DF* in an obstructed environment (Mavromatidis, Marsault, and Lequay 2014; Li et al. 2017), as the calculation is only more complicated.

The International Commission on Illumination (CIE) recommends the use of *DF* as it is the simplest parameter to qualify the daylight gain in an interior space with openings and minimize its need for artificial lighting. We focus only on the diffuse radiation of the sky, because the *DF* is theoretically invariant with the orientation of the building and depends only on the openings and the position of masks in the area of visibility of the sky (any natural or artificial element, near or far, likely to obscure the sky at any time of day). However, while producing a little initial assessment of the luminous comfort, *DF* is a static metric based on worst-case luminous conditions – and thus underestimates the actual daylight illuminance through the openings – compared to other more recent daylight metrics (Guan 2020).

Among them, three improved metrics in particular stand out, which inherently depend on the climatic conditions of the location and orientation of the building under study, significantly affect the luminous comfort of the occupants, and are often used jointly in optimization phases, for example in (De Luca et al. 2019; Peters et al. 2019; Lin and Tsay 2021; Nourkojouri et al. 2021; Le-Thanh et al. 2022):

- Useful daylighting (UDI): introduced in (Nabil and Mardaljevic 2006) as the percentage of annual occupancy time where the level of illumination provided by natural light alone is within a predetermined tolerance interval. It uses a meteorological dataset incorporating hourly sun and sky conditions. It is the most basic indicator, since it allows us to value building systems that favour natural lighting over artificial lighting without becoming a significant source of glare (Wienold 2009).
- Spatial Daylight Autonomy (sDA): represents the fraction of occupied space that receives at least the

minimum required illuminance (300 lux) for at least 50% of the annual occupied hours. sDA evaluates the daylight potential of different work environments through dynamic simulations.
- Annual sunlight exposure (ASE): fraction of the occupied space that receives at least 1000 lux during at least 250 occupied hours. ASE is often introduced to balance daylight availability and glare risk inside buildings.

For eaxample, in (Dogan and Park 2017) the authors propose a framework for assessing daylight in a residential living space over a one-year period. It consists of three sub-measures: SDA, direct light access (DLA), and an overall residential daylight score (RDS). It is intended to help quantify the daylight autonomy and sunlight access of existing buildings in the design phase.

- b) the availability of appropriate lighting levels for artificial lighting, generally in accordance with the minimum levels set by international standards and recommendations according to the type of activity. The designer can use in the sizing phase of the project a normative aspect related to the comfort of work and associated with: the percentage of area with a $DF > 2\%$ (*DF2*) and the Annual Solar Exposure (ASE). For high-performance office working conditions, the optimal range of use is: $DF \geq 2\%$ over 80% of the surface area of the primary zone in 80% of the premises (by area), and limited in general to 5%. This area corresponds to 4.7 m distance from the main window for a ceiling height of 3 m (Naeem and Wilson 2007; Si et al. 2014). Two other indicators have been designed: *DF2* / *DF* which expresses the abundance and homogeneity of natural lighting, and *DF2* / ASE which expresses the abundance of light according to solar gain (Guan 2020). This 5% threshold is emblematic because if a room has an average daylight factor of 5% or more, then electric lighting will most likely not be used during the day.

- c) calculations in the design phase: here, *DF* is useful to the architect to estimate the natural light contribution of his project (even though he does not know all the characteristics, especially concerning materials), to orient his building, to minimize the need for artificial lighting, and to obtain a correct sizing of the apertures for each façade. Indeed, the reduction of window area plays a key role: even if it does not deteriorate daylighting performance, it can improve thermal insulation and reduce the need for cooling (Cheung and Chung 2005). The light performance can be controlled in different ways: by acting on the reflectance factors of the exterior and interior surfaces, by varying the shape and size of the openings thus modifying the visible sky angle and the amount of incoming reflected light.

Hence the interest of generative software that anticipates these aspects, such as EcoGen2.1 (Marsault and Torres 2019) and SpaceMaker (SpaceMaker software), and that are capable of examining in only a few seconds hundreds of optimization variants of the solar potential for a project, contrary to others that are rather calculation or verification tools, such as VeLUX (certainly dedicated to the upstream phase), Autodesk Insight, DIALux, IES-VE, EnergyPlus, Radiance, Daysim, ArchiWizard or Diva-for-Rhino (that improved in ClimateStudio) which can be called to the other phases to perform complete analyses, but much more slowly. They are also used for daylighting performance prediction and energy savings potential analysis in energy efficient building topologies, independent of construction expenses. See (Ahmad et al. 2020) for a comprehensive comparison of these software packages under various obstructed, covered and uncovered skies. This unprecedented access to high-quality daylight analysis at the earliest stages of design gives architects and planners some of the answers they need, and enables them to meet the challenge of optimizing daylight capture in dense urban environments.

2.2. Daylight models and simulations

Daylighting modeling has grown rapidly in the last two decades, allowing the generation of photorealistic computer images, but also numerical simulations of daylight levels in living spaces during the design phases of architectural or construction projects, with an accuracy depending on factors such as building geometry, calculation method, sky model and surface properties.

Predicting the daylight level at any point in a built interior space is fundamental to daylighting analysis. Solar radiation and outdoor illuminance, especially on vertical surfaces, are critical to the design of energy-efficient buildings and daylighting systems (Li, Lau, and Lam 2005). Numerical techniques for determining the sky component and daylight reflected from surrounding buildings and ground surfaces have also been studied in detail in (Li, Chau, and Wan 2013).

A first analytical formula of the average *DF* in a room was developed in (Crisp and Littlefair 1984), under four assumptions: diffuse overcast sky, vertical openings, uniform wall reflection and empty room. It took into account the total surface of the internal walls of the room, the surfaces of the glazed openings with their transmission coefficient, the diffuse reflection of the walls and the angle *A* of the sky visible from the glazed openings. This formula provided an approximation on average 30% higher than the *DF* (Naeem and Wilson 2007), because it was sensitive to variations in the calculation of *A* and above all did not

take into account the angular height which has a strong influence on the luminance of the perceived sky.

The difficulties in predicting daylight in an indoor space, due to the non-linearity of the physical phenomena involved, have opened the way to the use of linear and non-linear metamodels.

2.2.1. Models improvements

In order to overcome the shortcomings of the *DF* metric – and in particular to account for orientation in order to take better advantage of the daylight – some researchers have designed variations or extensions of the original model, mainly for simplified convex volumes, without external mask or proper shading. In this vein, the paper (Mebarki et al. 2021) presents a series of nonlinear statistical metamodels that improve the academic daylight factor model to account for different glazing types and orientations, geographic location of the building, and sky and time of day conditions, in order to subsequently optimize window size and building energy demand. The produced metamodels incorporate an orientation factor, a cloudiness factor, and a luminous efficiency.

Since the manipulation of arbitrary shapes is always a challenge for building performance metamodeling, especially in the early stages which often favour simple shapes, other researchers have relied on intermediate feature design (Lin and Tsay 2021; Le-Thanh et al. 2022) combined with machine learning. The paper (Le-Thanh et al. 2022) focuses on a machine learning approach to determine the relationship between sensors and light obstacles in a voxel-like building environment (22 m x 10 m x 4.2 m). An Artificial Neural Network (ANN) is trained and used to predict the UDI based on the results of many simulations. By modifying the geometry of a parametric façade type and performing a daylighting simulation, the authors of (Lin and Tsay 2021) were able to generate eleven intermediate features (six for positions, five for shading) in addition to the sDA/ASE values, as new input parameters to train the ANN, used to characterize daylight penetration performance quite finely in a large majority of geometric configurations.

2.2.2. The use of machine learning in metamodels

A recent state of the art of the use of machine learning for building (Hong et al. 2020) shows many contributions. Globally, the techniques used range from (multi)linear regressions to non-linear regressions, including chaos polynomials (Xiu, Karniadakis, and Xiu 2002), and finally to artificial neural networks (ANN), whose first uses in the field of building simulation date back about 15 years. Constructed via DOE (design of experiments) methods (Goupy 2017), fractional factorial designs were mainly used in the past for energy consumption issues in building applications (Mavromatidis, Marsault, and Lequay 2014; Nault 2016; Catalina, Virgone, and Blanco 2008; Catalina, Iordache, and Caracaleanu 2013).

More specifically, a large number of recent studies have focused on the use of machine learning to predict the internal daylighting of a living space (Mavromatidis, Marsault, and Lequay 2014; Walger da Fonseca and Ruttkay Pereira 2021; Lin and Tsay 2021; Nourkojouri et al. 2021; Le-Thanh et al. 2022; Hong et al. 2020; Kazanasmaz, Gunaydin, and Binol 2009; Ayoub 2020; Zhou and Liu 2015; Radziszewski and Waczynska 2018; Lorenz et al. 2018; Janjai and Plaon 2011). They show the potential of a large pannel of algorithms to automatically and accurately learn the interactions between sunlight and building parts. The parametric variants for constituting the datasets are chosen among the room dimensions, the reflectance of the interior surfaces, the window dimensions, the number of windows, the room orientation, the type and the shading states.

Now, Artificial Neural Networks are becoming increasingly effective in simulating building energy performance, thanks to deep learning advances. First used for solar radiation prediction, either in terms of global radiation or solar irradiation at the building surface, and its correlation with different types of sky (Li, Chau, and Wan 2013; Janjai and Plaon 2011; Loutfi et al. 2017), ANN are capable of finely approximating any function, especially non-linear, provided that their architecture is well designed and that they have sufficiently large datasets (often requiring a great deal of effort to build up the machine learning process). Since then, their use has been steadily expanding to many other calculations in Building Simulation, for example to obtain the distribution of natural and artificial illuminance in an office using daylight simulations and a limited number of sensors or in-situ measurements (Si et al. 2014; Kazanasmaz, Gunaydin, and Binol 2009), or the analysis of daylight availability (Mavromatidis, Marsault, and Lequay 2014; Ayoub 2020). Luminous comfort and daylighting performance assessment use vision algorithms for automatic and large-scale assessment of the visual environment of buildings and cities, taking advantage of the latest machine learning techniques (Zhou and Liu 2015); or for predicting daylight autonomy levels in indoor spaces as an alternative to computationally expensive daylighting simulations (Radziszewski and Waczynska 2018; Lorenz et al. 2018). A recent neural meta-modeling of daylighting inside an office (Katsanou, Alexiadis, and Labridis 2019) takes into account the evolution of internal lighting conditions and user actions in a work environment with blinds (a study involving three offices located in the same university

building was presented, based on simulations with the DIALux software DIALux software). His models integrate daylight, individual user comfort and energy consumption. Lastly, (Walger da Fonseca and Ruttkay Pereira 2021) describes an ANN as a robust metamodel for a fixed-size voxel of 16 m x 8 m. In (Nourkojouri et al. 2021), a dataset is derived from 3000 simulations developed from Honeybee for Grasshopper for a side-lit voxelized model. Five metrics are applied to evaluate useful illuminance, sDA and ASE, annual sun exposure, and quality of view.

But neural models have important limitations pointed out by many researchers and practitioners. First, unlike explicit algorithms such as decision trees, neural learning models are opaque, and it is difficult to determine causal relationships between variables from such models. In addition, it can be noted that a low-dimensional regression polynomial is always much faster to compute (on CPU and even on GPU) and to implement than a neural network (Catalina, Virgone, and Blanco 2008). In particular, it avoids the evaluation of a large number of activation functions and the delicate and sometimes time-consuming adjustment of a dozen hyperparameters such as the number of hidden layers, the number of neurons in each layer, the type of activation function and the dynamic learning rates. Finally, if one wants to finely control the parametric behaviour of the metamodel – which is often desirable in the design of building components – polynomial regression methods will be more adapted to this kind of adjustment, as Emilie Nault showed in her thesis (Nault 2016), by exploiting the "spatial daylight analysis" metric on typical morphological configurations (unfortunately not very generic, too simplified and with few or no hypotheses on the openings).

2.2.3. Back to regression metamodels

Among previous works, a first metamodel of the *DF* inside a parallelepipedic building was published in 2014 in (Mavromatidis, Marsault, and Lequay 2014). The authors focused on the development of a quadratic polynomial regression method to estimate fairly accurately – albeit at the early design stage – the daylight received inside a basic cuboidal volume named voxel, placed in a highly obstructed urban environment, when some problem data are not precisely determined (positions and dimensions of glazed surfaces, material types, opacity levels, …). Their major contribution was to take into account simplified parametric masks for each opening, allowing the consideration of real situations quite varied: each face i with an opening rate w_i had at most one rectangular mask (h_i x l_i), centred, located at distance d_i from the floor-to-ceiling window bay (Figure 1; also used in Lin and Tsay 2021).

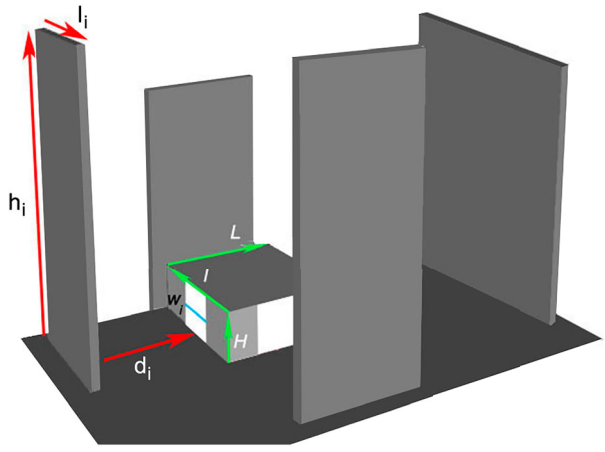

Figure 1. Centred rectangular masks (d_i, l_i, h_i) for a voxel of dimensions (H, L, l, w_i).

The major weaknesses of their model were:

1) to freeze the voxel dimensions ($H = 4$ m, $L = 12$ m, $l = 10$ m); so with no answer for a voxel of any dimensions, as done in other papers (Marsh and Stravoravdis 2017; De Luca et al. 2019; Le-Thanh et al. 2022);
2) to restrict the parametric domain for masks (D), especially in depth (while maintaining sufficient power to cover the visible sky).

$$d_i \leq 20\,m, l_i \leq 20\,m \text{ and } h_i \leq 50\,m \qquad \text{(D)}$$

These limits were justified by the need to restrict the number of simulations to complete the calculations in a given time (design of experiments of 284 scenarios of numerical simulations of the Box–Behnken type (Box and Behnken 1960), which was already expensive in terms of calculation time).

The authors used the DIALux software (DIALux software) with the CIE 110–1994 clear and overcast sky model (http://www.dial.de/DIAL/fileadmin/download/DIALux/wissen\Dx4_Rechenkern_eng.pdf) equipped with the Krochmann zenith luminance (Robert 1979). The illumination reception plane was set at 0.8 m from the ground and included 100 uniformly distributed targets (also called sensors). This metamodel, which we will call by now DF_{2014}, sought to express analytically the *DF* of a single room of fixed size as a function of 17 independent variables: centred aperture rate in facade (sufficient approximation in the sketch phase), type of environment (atmospheric pollution = *env*), dimensions and depth of the centred rectangular masks (Figure 1). A sensitivity analysis allowed to detect the main couplings among the 170 polynomial variables and to eliminate those having a negligible influence (among others those related to the couplings between facades), to

keep only 45 (to be discussed in 3.1.1 section). Finally, in order to validate the accuracy and stability of the adjustment model, a correlation analysis between DIALux calculations and the model's estimates was carried out thanks to statistical measurements of the error committed ($R^2 = 0.9551$, BIAS = 0.001413, RMSE = 0.1589) and classical tests (CooK distance, Henry plot, Box–Cox plot) provided by Design Expert software. These results showed that the mean square error caused by the simplification was acceptable under most conditions, and allowed the metamodel to be used with confidence. Thus, in the sketch phase of an architectural project, this model reduced the complicated calculation of the *DF* for a fixed-size cuboid housing unit by providing a sufficiently accurate and extremely fast answer, given acceptable simplifying assumptions in geometry and materials. It helped the designer by proposing an 'equivalent glazed area' for each wall, a sort of guide for placing openings on the facades at his convenience, according to the use of the premises.

2.3. Towards realtime physical simulations

The fundamental concepts underlying most physical calculations are well known. There are essentially four methods for simulating the spatial distribution of diffuse illuminance in a room (Marsh and Stravoravdis 2017): split-flux, radiosity, ray-tracing and photon mapping methods, the first being the least computationally expensive. In the BS community, daylighting simulation and global illumination computation is usually performed using directly or indirectly the Radiance suite, a robust simulation engine widely experienced by practitioners and researchers, and implemented in a large pannel of tools based on ray tracing (IES, DAYSIM, DIVA for Rhino, ClimateStudio, late Ecotect, …).

Until ten years ago, daylighting simulations could only be fully realized on CPUs (Woop, Schmittler, and Slusallek 2005), even if functional prototypes on GPUs already existed in graphics research laboratories. The last few years have seen the democratization of deep GPU programming with architectures more adapted to ray tracing and path tracing, notably from Nvidia (CUDA-based Optix (Parker et al. 2010), RTX cards since 2019). By means of a new expertise in programming these processors, researchers have been able to obtain significant acceleration of the calculation times of many luminous quantities. It is certain that obtaining on recent GPUs computations in interactive time (currently a bit less than half a second per evaluation) opens the door to interactivity in a large number of numerical design applications, without however being considered fully as real time computation.

In a series of five papers between 2014 and 2017 (Jones and Reinhart 2015; Jones and Reinhart 2016; Jones and Reinhart 2017; Jones and Reinhart 2014; Jones and Reinhart 2014), Jones and Reinhart overwhelmingly improved the performance of several open source modules (*rpict*, *rtrace_dc*, *rvu*, *rcontrib*) in the Radiance suite and grappled with the technical challenges of parallelism and GPU programming to accelerate daylight simulations. (Jones and Reinhart 2015) describes the development of a tool for fast *DF* calculation using a GPU. The tool is an adaptation of *rtrace_dc*, the executable used by DAYSIM to compute daylight coefficients, written using OptiX, a library created by Nvidia for ray tracing on GPUs (Parker et al. 2010), and widely used by the BS community. The simulations show a relative error of less than 6%, which is acceptable for early design analysis. The authors then created GPU-accelerated parallel versions of *rtrace*, *rpict* (Jones and Reinhart 2014) and *rvu* (Jones and Reinhart 2016) that boost Radiance's ray tracing functionality and lead to the Accelerad tool. In (Jones and Reinhart 2014), this transition from the CPU to GPU provided up to a twenty-fold performance increase. In (Jones and Reinhart 2017), they focused on parallelizing the latest ray tracing programme, *rcontrib*, to allow easier access to sDA and ASE daylight measurements. Finally, (Jones and Reinhart 2014) implements irradiance caching on the GPU and allows further speed-up of the Radiance algorithms by selectively reusing ambient values from previous calculations. Coupled with code optimization and OptiX implementations on Nvidia RTX cards, the authors lead to a hundred-fold performance improvements in Accelerad-RT, their latest interactive interface for real-time daylighting, glare and visual comfort analysis, which uses progressive path tracing to provide daylighting simulation results in real time with validated accuracy. As in (Marsh and Stravoravdis 2017), the tool is interactive and responds to changes made by the user in the underlying geometric and material models. Their codes are available online.

Other recent works have exploited techniques of hemispheric subdivision of the sky dome into discrete elements (each with its own luminance) to finely integrate the luminous fluxes from the sun and the diffuse sky in their models and simulations. Tables or lists of indirections (coded on the CPU or in textures on the GPU) allow to access very quickly to the discretized elements visible from each point of interest (sensors) of the studied location (Marsault and Torres 2019; Marsh and Stravoravdis 2017) and/or its outer envelope (Marsault and Torres 2019). In (Marsh and Stravoravdis 2017), the authors present a simulation tool initially implemented on a GPU to compute the spatial distribution of daylight factors in a rectangular room via the split flux method.

In a first step, they justify the porting of analytical computations on GPU to create a highly dynamic and interactive building simulation environment and manipulate daylighting parameters in real time. They finally show that their latest approach, which takes advantage of the dynamic optimization capabilities of JavaScript code in current browsers, avoids direct programming of a GPU and exhibits very similar execution times on a CPU. In (Marsault and Torres 2019), the authors describe EcoGen2, a software where the evaluation and optimization of the overall solar gains received by the built envelopes, conducted in realtime on the scale of a block or a small district, are in line with the need to pool energy. They are carried out for solar gains and shading masks, partly pre-calculated on the envelopes of the sites buildings interacting with each other from the point of view of light.

3. Originality and novelty of our approach

In previous works, achieving interactive computation (2-orders-speedup compared to usual softwares) has been especially tackled by Jones and Reinhart (Jones and Reinhart 2015; Jones and Reinhart 2016; Jones and Reinhart 2017; Jones and Reinhart 2014; Jones and Reinhart 2014), Marsh and Stravoravdis (2017) for computation of illuminance indicators in indoor out outdoor scenes, almost reaching realtime rates, thanks to entensive use of the GPU.

Our main goal was to achieve realtime computation for illuminance indicators, especially for the daylight factor, without necessarily using an expensive GPU. Our research has addressed this objective by means of a hybrid computation both based on physical and statistical modeling, and on a physical-based computation engine specifically used for the needs of generative design. This is our main contribution.

With regard to rapid calculation of light indicators (DF, sDA, ASE, UDI), modular buildings have poorly been treated by previous researchers (except in Marsault and Torres 2019; Peters et al. 2019). Most have focused on offices or living units (Jones and Reinhart 2015; Marsh and Stravoravdis 2017; De Luca et al. 2019; Walger da Fonseca and Ruttkay Pereira 2021; Lin and Tsay 2021; Nourkojouri et al. 2021; Mebarki et al. 2021) based on simple shapes (like boxes or cuboids), often convex, of fixed size and with no or little external occultations nearby.

We consider here a more elaborate building morphology, with several floors of different heights, each floor having its own relative rotation (5% to 10%). The basic brick of this construction is a parallelepipedic module called voxel, with parametrizable dimensions but identical for a given floor and with facades potentially tiltable towards the sky. Different uses of this parametric morphotype are modern aggregated architectures, non convex corbel buildings and twisted towers, which widen the field of design possibilities.

Our paper deals with the very fast computation of *DF* for this specific case, and we are proud to achieve computations of the ms order per solution on recent CPUs. It is divided in two parts: the first one describes an approximation statistical metamodel for a basic voxel with a few parameters; the second one shows its integration in a generative design framework able to estimate in real time the parameters of all voxels constituting a modular building generated on the fly (section 4).

Our approach respectively benefits from: 1) a hybrid validated statistical metamodel for *DF* based on a couple of regression equations (section 3) ; 2) the contributions of *Target Computing*, a physics engine developed from 2014 to 2016 for the realtime evaluation of light interactions in urban scenes, promoting solar courtesy on the neighbourhood.

The *Target Computing* engine is derived from a three-year research project on fast light calculations and illuminance for modular buildings within their built environment (still unpublished for software protection and patent reasons, but briefly mentioned in Marsault and Torres 2019). It fully takes into account in the computation: a) annual climate-based daylight fluxes (direct and diffuse irradiations, reflections from the ground); b) all shadow and masking effects resulting from the built environment. A pre-computation optimized step – which takes a few seconds at the begining of the generative design process – makes them accessible in realtime via a powerfull CPU caching mechanism which avoids ray casting, based on a a quick access structure made of hierarchical visibility sensors and occulting mask lists. With a total integration in the framework of EcoGen2 (Marsault and Torres 2019), no complex software suite is required. Totally CPU-based, it does not require any expensive hardware like recent GPUs, nor CUDA code adaptation over time (often leading to compatibility issues). It leaves the GPU power for other tasks, like Dynamic Fluid Computation more and more required in modern BS simulations.

3.1. Materials and methods for a generalized and hybrid metamodel

This section describes in detail how we have generalized and enriched the previous metamodel: DF_{2014} (Mavromatidis et al. 2014), making it more robust and versatile.

3.1.1. Improvement of the previous DF_{2014} metamodel

First, beyond the limits previously mentioned, and even while considering good results in the variance analysis of

the regression process, the DF_{2014} metamodel, like most regression models, does not preserve the direction of physical variation with the input variables (d_i, l_i, h_i, w_i). The more parameters associated with these variables, the more likely this is to occur. This is particularly troublesome when the model is to be used for the purpose of sizing building components. For example, the EcoGen software that we have used to implement our new hybrid metamodel relies on mask size estimates that are accurate enough to provide the architect with solutions that are comparable to each other once the current voxel dimensions are fixed. In this case, *DF* should at least satisfy the following constraints:

$$\forall_i \leq 4 : \frac{\partial DF}{\partial w_i} > 0,\ \frac{\partial DF}{\partial d_i} > 0,\ \frac{\partial DF}{\partial l_i} < 0 \text{ and } \frac{\partial DF}{\partial h_i} < 0 \quad \text{(eq.A)}$$

However, the respect of the 16 inequalities (eq.A) is not possible by maintaining the number of coefficients (45) of DF_{2014}. It has been shown that it is necessary to add couplings of variables not retained at the time by Design Expert's variance analysis, and to have the same number of coefficients (18) in each cardinal direction, for reasons of isotropy of the diffuse sky flux. The original experimental design of 284 scenarios was maintained, and we used a constrained genetic optimization algorithm developed in the laboratory to obtain an homogeneous quadratic polynomial (eq.B):

$$DF_{2014}(env,\ \{w_i, d_i, l_i, h_i\}_{i=1\ to\ 4}) = \sum_{i=1}^{4}\sum_{j=1}^{18} coeff_{ij}.weight_{ij} \quad \text{(eq.B)}$$

with 72 coefficients $coeff_{ij}$ and their weights detailed in Table 1, *env* being a classical atmospheric pollution parameter in [0.55; 1.0].

As in the previous model, the absence of coupling between facades allows an additive calculation of the *DF* in four separate cardinal polynomials (Table 1, $coeff_{1\,to\,4}$), that should be factorized to optimize the calculation, and whose application is conditioned to the effective presence of an opening in each respective direction.

Table 1 is of great importance in a buiding design, because it provides an 2-order polynomials that respects the variations of *DF* with the input parameters, which unfortunately is not often the case with metamodels.

The statistics of this revisited model are significantly improved over the previous one, except for BIAS (which was expected): $R^2 = 0.981294$, $BIAS = -0.00194364$; $RMSE = 0.085657$.

Finally, the DF_{2014} polynomial, although evaluated under the assumptions of diffuse sky isotropy, still exhibits a North/South and East/West skewness due to the native difference between its length and width. Our new metamodel, in fact, slightly takes into account the orientation in a generalized modelization of the *DF* which by essence does not: here, by slightly favouring the South in sub-polynomial 3. During its use (see section 4), this leads us, for the sake of compatibility, to assign the face indexes of DF_{2021} according to the orientation ratio *L*/*l*.

3.1.2. Assumptions

We retain the description of the voxel geometry, simplified aperture masks and material characteristics described in (Mavromatidis, Marsault, and Lequay 2014). A description of the voxel geometry and simplified aperture masks can be found in Figure 1. The aperture rates (w_1, w_2) refer to *L* and (w_3, w_4) to *l* (Figure 3). A uniform interior material (Lambertian white, average reflectance = 27%) is used; the reflectance factors of the surfaces are set to 0.7 for

Table 1. The 72 coefficients of the revisited quadratic DF_{2014} model for a 12 × 10 × 4 m voxel, respecting the physical variation direction of the parameters (d_i, l_i, h_i, w_i). Its additive nature results in 4 separate cardinal polynomials (4 columns for analytical $coeff_{1\,to\,4}$ and associated weights – 1 = East, 2 = North, 3 = South, 4 = West).

$coeff_1$	$weight_1$	$coeff_2$	$weight_2$	$coeff_3$	$weight_3$	$coeff_4$	$weight_4$
$const_1$	1.940535049	$const_2$	1.756957016	$const_3$	2.073638279	$const_4$	1.598245029
env	−0.57308566	env	−0.678041877	env	−0.772902892	env	−0.434653123
d_1	−0.042805198	d_2	0.008171806	d_3	0.018155757	d_4	−0.068314636
l_1	0.01262298	l_2	0.020094472	l_3	0.012831581	l_4	0.024866528
h_1	−0.034532866	h_2	−0.021629955	h_3	−0.043312373	h_4	−0.016547323
w_1	−0.000732345	w_2	−0.011947998	w_3	0.005191148	w_4	−0.001094947
$w_1 * l_1$	−0.000832197	$w_2 * l_2$	−0.00067826	$w_3 * l_3$	−0.001050193	$w_4 * l_4$	−0.000655631
$w_1 * h_1$	−0.000254099	$w_2 * h_2$	−0.000203478	$w_3 * h_3$	−0.000222181	$w_4 * h_4$	−0.000175151
$w_1 *$ env	0.035653998	$w_2 *$ env	0.051482381	$w_3 *$ env	0.037755804	$w_4 *$ env	0.027325855
$d_1 *$ env	0.072445521	$d_2 *$ env	0.077190884	$d_3 *$ env	0.049524365	$d_4 *$ env	0.098760193
$d_1 * d_1$	−0.000503704	$d_2 * d_2$	−0.001839801	$d_3 * d_3$	−0.001590086	$d_4 * d_4$	−0.000329428
$d_1 * l_1$	0.003440919	$d_2 * l_2$	0.00253071	$d_3 * l_3$	0.002726205	$d_4 * l_4$	0.002201249
$d_1 * h_1$	0.00117942	$d_2 * h_2$	0.000933629	$d_3 * h_3$	0.001269768	$d_4 * h_4$	0.000732485
$d_1 * w_1$	0.000510019	$d_2 * w_2$	0.0005042	$d_3 * w_3$	0.000663593	$d_4 * w_4$	0.000508565
$l_1 *$ env	−0.105819914	$l_2 *$ env	−0.103307977	$l_3 *$ env	−0.103161009	$l_4 *$ env	−0.088049976
$h_1 * l_1$	−0.000511158	$h_2 * l_2$	−0.001091958	$h_3 * l_3$	−0.001724797	$h_4 * l_4$	−0.001106318
$h_1 * h_1$	0.000318152	$h_2 * h_2$	0.000126663	$h_3 * h_3$	0.000518801	$h_4 * h_4$	9.69688E-05
$l_1 * l_1$	0.000117789	$l_2 * l_2$	0.000332892	$l_3 * l_3$	0.000476345	$l_4 * l_4$	8.22159E-05

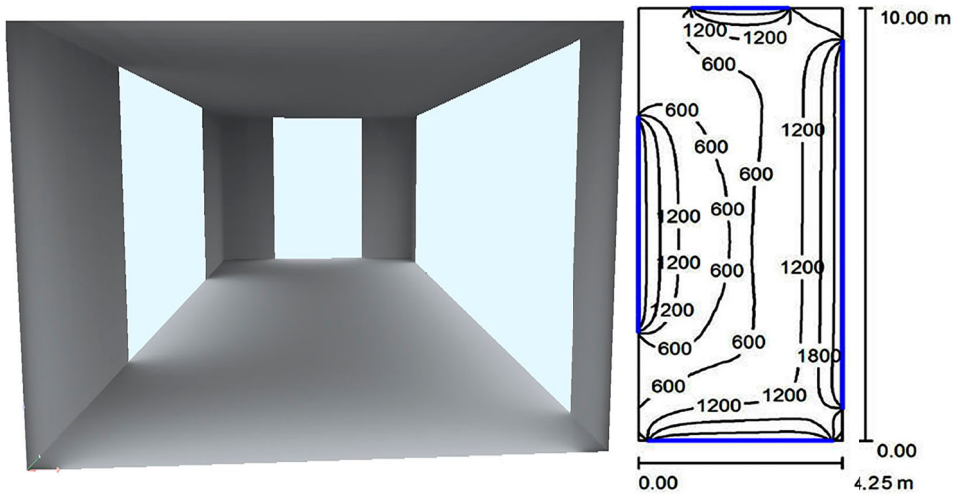

Figure 2. Example of simulation under DIALux of the calculation of *DF* and isolux curves for a voxel with 4 openings.

ceilings, 0.5 for walls and 0.2 for floors. The average *DF* is calculated by DIALux on a work surface (x, y) of the same area as the room S = *L.l*, located at a height $h = 0.8$ m from the floor and finely sampled, which allows to obtain precise isolux curves (Figure 2).

We now describe the method used to generalize the DF_{2014} metamodel for a voxel of any dimensions, allowing for a wide usage domain (V).

$$1 \leq L \leq 50m,\ 1 \leq l \leq 50m \text{ and } 2 \leq H \leq 7m \quad \text{(V)}$$

First, let us clarify that we did not want to redo all the regression calculations of the DF_{2014} model with three additional variables (*H*, *L*, *l*), which would have required thousands of new Box–Behnken simulations.

Initially, we focused our attention on a first new metamodel, DF_{2021}, based on the 7 voxel-specific dimensional variables (*H*, *L*, *l*, w_1, w_2, w_3, w_4), without considering masks. A new design of experiments of 91 simulations performed with DIALux was obtained by sampling uniformly on (V) the 6 variables (*L*, *l*, w_1, w_2, w_3, w_4) for each integer value of *H* between 2 and 7 m. Then we show (in section 4) how to integrate the masking effects provided by DF_{2014}.

3.2. Physical modeling

Unlike physics-based models, data-driven approaches – such as statistical modeling – do not explain the links between inputs and outputs. They simply optimize correlations. In this case, we will build a new metamodel, called hybrid, because it calls upon a statistical model to optimize specific parameters of a physical model. Obviously, in the coefficients of the metamodel are also hidden physical parameters: nature of materials, reflectance factors, types of glazing and impact of reflections between internal walls of the room. This avoids describing them specifically later.

Thanks to physical modeling, we were able to build an extension of the DF_{2014} metamodel, minimizing the number of new simulations with DIALux: 1) to take into account variable dimensions (*H*, *L*, *l*) of a voxel in the (V) domain; 2) to take into account the possible tilt of the faces towards the sky; 3) to extend the domain of validity of the masking parameters (D) on each face. Normally, the estimation equations are invalid if one or more parameters are beyond the learning domain of the model (here D). But here, it is quite easy to get back to this when required, using a calculation based on the equivalent luminance (section 4.6).

Let us start by explaining in six points the original idea of the DF_{2021} model and its preparation:

1) Incoming light flux

First of all, we express the fact that the luminous flux Φ_E entering the room is received by all openings and does not depend on their orientation (uniform diffuse sky in azimuth). *K* designating a constant, this flux can therefore be expressed as a function of the opening surfaces by (eq.C):

$$\Phi_E = K.H.((w_1 + w_2).L + (w_3 + w_4).l) \quad \text{(eq.C)}$$

2) Academic expression of the DF

By definition, the daylight factor is expressed as an illuminance ratio (eq.D).

$$DF = \frac{E_{xy}}{E_{ext}} = \frac{E_{xy}}{11432} = \frac{\left(\frac{\Phi_{xy}}{S}\right)}{11432} \quad \text{(eq.D)}$$

where $E_{ext} = 11432$ lx is the outdoor illuminance measured (by DIALux) on a diffuse open horizontal surface and E_{xy} is the illuminance measured on the work surface inside the room.

3) Introduction of a flux ratio

Since there is no formula for calculating the flux Φ_{xy} received on the work plane, we introduce (in eq.E) the ratio p_{xy} corresponding to the contribution of flux Φ_{xy} to the incoming flux Φ_E.

$$\Phi_{xy} = p_{xy}.\Phi_E \qquad \text{(eq.E)}$$

By entering the constant K from (eq.C) into p_{xy}, we can write:

$$DF_{2021} = p_{xy}.\frac{C_1}{E_{ext}} \qquad \text{(eq.F)}$$

With:

$$C_1 = H.((w_1 + w_2)/l + (w_3 + w_4)/L) \qquad \text{(eq.G)}$$

4) Physical constraints to satisfy

Contrary to the usual practice which favours polynomial regressions directly on the variables of the problem (even if it implies losing the physical meaning), the analytical form of DF cannot be simply a polynomial of (H, L, l, w_1, w_2, w_3, w_4), whatever its degree. Indeed, an elementary physical reasoning imposes to satisfy: the growth of DF with w_i (eq.A) and the following boundary conditions (eq.H) according to the variations of the parameters H, L and l:

$$\lim_{H\to 0} DF = 0 \text{ and } \lim_{H\to+\infty} DF > 0 \text{ (bounded)}$$

$$\text{if } w_1 + w_2 > 0 : \lim_{L\to 0} DF > 0 \text{ if } w_3 + w_4 > 0, \text{ and 0 if not}$$

$$\text{if } w_3 + w_4 > 0 : \lim_{l\to 0} DF > 0 \text{ if } w_1 + w_2 > 0, \text{ and 0 if not} \qquad \text{(eq.H)}$$

$$\text{if } w_1 + w_2 > 0 : \lim_{L\to+\infty} DF > 0 \text{ if } w_3 + w_4 > 0, \text{ and 0 if not}$$

$$\text{if } w_3 + w_4 > 0 : \lim_{l\to+\infty} DF > 0 \text{ if } w_1 + w_2 > 0, \text{ and 0 if not}$$

5) First expression of DF_{2021} at order 0

If we use homogeneous ratios of the voxel dimensions (H, L, l) in the expression of DF (of the type H/L, L/l, l/H, Ll/H^2, …), it is easy to check that it is possible to satisfy the boundary conditions of (eq.H). Moreover, we will show by physical modeling that p_{xy} is expressed as the inverse of a function f involving such ratios (eq.I).

$$p_{xy} = \frac{1}{f(\frac{H}{L}, \frac{L}{l}, \frac{H}{l}, \ldots, w_1, w_2, w_3, w_4)} \qquad \text{(eq.I)}$$

We construct this function f by expressing the fact that Φ_{xy} is related to the distribution of light energy Φ_E over all interior surfaces of the voxel. These surfaces are divided into apertures and opaque surfaces, depending on whether we consider the floor, ceiling or walls. There are two types of interaction between them: direct (order 0) or and indirect (higher order).

We first tested a model at order 0, neglecting the inter-reflections. In this case, the receivers (opaque parts of the walls) receive only the direct energy of the emitters (openings), and a slight calculation from equations (C, F, G) allows to obtain a simplified model (eq.J) with only 4 parameters (a, b, c, d):

$$p_{xy} = \frac{L.l}{a.L.l + b.H.L.(2 - w_1 - w_2) + c.H.l.(2 - w_3 - w_4) + d} \qquad \text{(eq.J)}$$

A linear regression on 1 / p_{xy} over the dataset leads to the estimation of these parameters ($a = 6.5318604$, $b = 1.41228204$, $c = 0.89791208$, $d = 10.0547822$), with a poor result (on a validation sample of 31 cases) for $R^2 = 0.793769$, even if RMSE = 0.154933 is more than correct and BIAS = 5.9476e-17 is excellent.

6) Finalized expression of DF_{2021} at order 1

Moving to order 1, we complete the previous model by introducing necessary couplings between surfaces – not present in (eq. J) nor in the previous DF_{2014} model – and thus we obtain a different analytical form. For this purpose, we specify that the flux received on the working plane is equal to a weighted sum of direct (eq.C) and indirect fluxes.

The calculation at order 0 for the direct fluxes involves the C_1 coefficient (eq. G) and a constant ($C_0 = 1$) that we will find in the first two lines of Table 2. Then, we describe the contribution of the indirect fluxes at order 1 by the sum of the interactions between the 4 emitters (direct sources = openings) and the 6 receivers (opaque parts of the walls + floor + ceiling). In a classical way, in the hypothesis of Lambertian materials, the contribution of each indirect flux i is can be expressed (eq. K) as the product of the interacting surfaces weighted by the inverse square of their average inter-distance d_{ij}:

$$_{\phi i\to j} = X_{ij}.\frac{E_i.R_j}{d_{ij}^2} \qquad \text{(eq.K)}$$

Table 2. The hybrid metamodel DF_{2021} (eq. M) described by its 17 analytical parameters C_i and associated weights X_i.

Analytical parameter C_i	Weight X_i
C_0 = constant	X_0 = 4,582470829
$C_1 = H.[(w_1 + w_2) / l + (w_3 + w_4) / L]$	X_1 = 1,979008817
$C_2 = H^2.L.w_1.(1 - w_2) / l^3$	X_2 = 0,004637097
$C_3 = H^2.w_1.(2 - w_3 - w_4) / (L^2 + l^2)$	X_3 = 4,012397217
$C_4 = H.L.w_1 / (l^2 + H^2)$	X_4 = -0,518663761
$C_5 = H^2.L.w_2.(1 - w_1) / l^3$	X_5 = 1,340735724
$C_6 = H^2.w_2.(2 - w_3 - w_4) / (L^2 + l^2)$	X_6 = 1,358627008
$C_7 = H.L.w_2 / (l^2 + H^2)$	X_7 = -0,867968571
$C_8 = H^2.l.w_3.(1 - w_4) / L^3$	X_8 = -0,668403779
$C_9 = H^2.w_3.(2 - w_1 - w_2) / (L^2 + l^2)$	X_9 = 1,138746826
$C_{10} = H.l.w_3 / (H^2 + L^2)$	X_{10} = -0,237174038
$C_{11} = H^2.l.w_4.(1 - w_3) / L^3$	X_{11} = -0,834442530
$C_{12} = H^2.w_4.(2 - w_1 - w_2) / (L^2 + l^2)$	X_{12} = -0,173008400
$C_{13} = H.l.w_4 / (H^2 + L^2)$	X_{13} = 1,359875791
$C_{14} = H.L.(2 - w_1 - w_2) / (H^2 + l^2)$	X_{14} = 0,639900967
$C_{15} = H.l.(2 - w_3 - w_4) / (H^2 + L^2)$	X_{15} = 0,327253327
$C_{16} = (L + l) / H$	X_{16} = 0,097624787

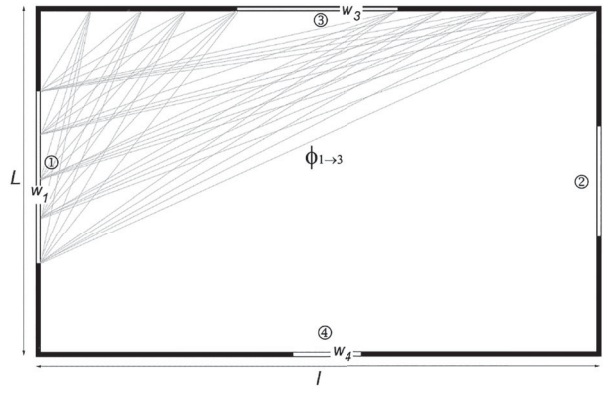

Figure 3. Interactions for computation of C_3 parameter in Table 2. For visual comfort, only the interactions in 2D between aperture 1 and opaque wall 3 are displayed; the same can be done for wall 4.

where E_i and R_j are the respective areas of transmitter i and receiver j, with the transmission rate ρ hidden in the weights X_{ij}.

Now, our goal is to estimate the X_{ij} weights. In order to limit the number of interactions (i→j), theoretically equal to 24 (4 emitters x 6 receivers), we use the isotropy of the diffuse sky and the symmetry of the voxel to group some terms together and obtain a lighter expression. Let's take an example: as displayed in Figure 3, coefficient C_3 in Table 2 gathers the $\phi_{1\to3}$ and $\phi_{1\to4}$ interactions of the aperture 1 (w_1) as a source and the two receiving opaque walls 3 and 4 (not including the openings 3 and 4: 2-w_3-w_4), with their average interdistance which roughly equals to $(L^2 + l^2)/3$. Then, (eq. K) simply leads to: $C_3 = X_3 \,.\, H^2 \,.\, w_1 \,.\, (2 - w_3 - w_4) \,/\, (L^2 + l^2)$. The other coefficients C_i are derived from similar calculations, so they do not need to be particularly detailed here (we just provide their analytical expressions in Table 2).

Adding a constant α and the term $\alpha \cdot C_1$ to (eq.K) to take into account the direct flux (order 0, previously explained), we obtain (eq.L).

$$p_{xy} = \frac{1}{\alpha_0 + \alpha_1.C_1 + \Sigma_{i,j}\, X_{ij}.E_i.R_j/d_{ij}^2} \qquad \text{(eq.L)}$$

Translating from (eq. L) to (eq.M) simply results from grouping C_k weights in generic variables X_i, then using (eq.F). We obtain the finalized expression of the daylight factor as a function of the 7 intrinsic dimension parameters ($H, L, l, w_1, w_2, w_3, w_4$) – excluding masks – expressed in percentage (eq.M).

$$DF_{2021}(H, L, l, \{w_i\}) = \frac{100.C_1}{\sum_{i=0}^{16} X_i.C_i} \qquad \text{(eq.M)}$$

Table 2 summarizes the analytical expressions and the weights of the 17 parameters C_i of this model. These weights are derived from a linear regression performed, as in the previous case, on 1 / p_{xy} with the Xlstat software. The quality of the model is considerably improved: $R^2 = 0.980355$; the other values remain quite acceptable: RMSE = 0.18983255 and BIAS = 0.00233791.

At this point – and this is a very good result for validation – it is important to note that this hybrid model has been carefully checked to ensure that the physical constraints stated in 4) are met: boundary conditions (eq.H) and increase of DF values as opening rates w_i increase (eq.A).

4. Integration of the new metamodel into a generative design software

In this section, we present the methodology used to optimize the daylighting potential of a building composed of multiple voxels, in the sketch phase of its design, within the framework of generative design. We first explain how to take into account masking effects with DF_{2021}. Then, we describe precisely the implementation of this integral metamodel for the computation of the DF performance in the generative design software EcoGen 2.1 (Marsault and Torres 2019), within which the morphogenesis of solutions is performed by optimizing arrangements of many voxels with a genetic algorithm (example in Figure 6).

4.1. Geometric similitudes

The computation of the DF of a unique voxel reveals some interesting geometric properties. First, if the interior illuminance were measured at the floor level, DF would be invariant by uniform homothety over the dimensions of

the voxel (eq.N).

$$\forall\lambda,\ DF_{floor}(\lambda H, \lambda L,\ \lambda l, \{w_i\}) = DF_{floor}(H,\ L,\ l,\ \{w_i\}) \quad \text{(eq.N)}$$

But since *DF* is measured at a constant height *h* with respect to the floor, it is not strictly invariant by homothety, or only if $H >> h$, which is uncommon. Moreover, from a practical point of view, arbitrary variations of the voxel dimensions rarely correspond to a uniform homothety. We then tried to study the behaviour of *DF* by associating a homothety ratio *i* to each dimension. More precisely, and in a rather intuitive way, we were interested in studying the ratio *R* (eq.O).

$$R = DF(\lambda_1 H, \lambda_2 L,\ \lambda_3 l, \{w_i\}) \,/\, DF(H,\ L,\ l,\ \{w_i\}) \quad \text{(eq.O)}$$

In the case where we only vary *H*, each opening having the same height *H* as that of the room (Figures 1 and 2), our simulations with DIALux show a quasi-linear relationship between the flow received on the work surface and the flow received by the floor: $\Phi_{xy} \cong \left(1 - \frac{h}{H}\right) \Phi_{floor}$. A similar conclusion can be found in (Naeem and Wilson 2007). But when the other two dimensions *L* and *l* are varied, it seems more difficult to obtain significant linear relations with *i*, as these vary according to the arrangement of the openings on *L* and *l*.

However – and this is the most important point of this section – we have highlighted a remarkable property by focusing on the variations of *R* with the introduction of masks, whatever the values of $i\lambda$. We simply found that by adapting the respective proportions of the rectangular masks (Figure 1) in a homothetic way between voxels of different dimensions, *R* reveals a quasi-stability property with or without masks. This important result will allow now to integrate in DF_{2021} the computation of masking effects on openings.

4.2. Integration of masking effects on openings

We will rather simply combine DF_{2021} (whose calculation is only related to the own geometry of the voxel) with DF_{2014} (translating precisely the masking effects of the openings for a voxel of known and fixed dimensions: 4, 12, 10 m).

Indeed, to obtain a generalized model, it is enough to apply the quasi-stability property of *R* stated previously to reduce the calculation of the *DF* of a voxel of dimensions (*H*, *L*, *l*) with masks to that of a reference voxel of dimensions (4, 12, 10 m). To obtain equivalent masks between these two voxels of different dimensions, we use the pseudo-homothetic coherence which allows to transform the parameters (d_i, l_i, h_i) into (d'_i, l'_i, h'_i) thanks to the respective ratios 12 / *L*, 10 / *l* and 4 / *H* (if $L > l$, and by permuting *L* and *l* in the opposite case). We finally obtain an expression for *DF* in the general case (eq.P) of a voxel of dimensions (*H, L, l*) with masks (d_i, l_i, h_i).

$$DF(H, L, l, \{w_i, d_i, l_i, h_i\}) = \frac{DF_{2021}(H, L, l, \{w_i\})}{DF_{2021}(4, 12, 10, \{w_i\})} . DF_{2014}(4, 12, 10, \{w_i, d'_i, l'_i, h'_i\}) \quad \text{(eq.P)}$$

4.3. Objectives and software choice

Computing the *DF* in realtime presents a certain difficulty, even for simplified voxel-based modeling. Moreover, the accurate estimation of local masks is in general an expensive problem (the built-up neighbourhood can be dense and irregularly distributed). Keeping in mind that a complete computation of the *DF* takes a lot of time (several tens of seconds on multi-core CPUs, and at most half a second on recent GPUs (Jones and Reinhart 2015; Jones and Reinhart 2016; Jones and Reinhart 2017)), we wish to achieve a realtime evaluation of the *DF* (about one ms). This is where the strength of the 'target computing' evaluation engine of the EcoGen2.1 architectural ecodesign software comes in, which allows access to precise data in terms of flux and masking for targets/sensors automatically placed on the envelope of a building and its close environment. The publication of this technique is still frozen under software protection since 2018 (France S.A.T.T. Pulsalys D01753). To simplify, each target/sensor has a very precise knowledge of its occultation environment, in the form of hierarchical lists of diffuse sky masks. When a sensor is placed on a window, it has access to the necessary data to instantly evaluate the luminous fluxes passing through this window. The counterpart of this very high efficiency is a complex C++ code mixing geometrical modeling, optimized algorithms and multi-core parallelism.

4.4. Hypothesis for a global DF computation

In a calculation during the sketch phase, one can neglect the depth transmission of interior light when several voxels are adjacent. First of all, at this stage of the project, we rarely know the plan of the interior spaces and doors. Second, in illuminance calculations, *DF* is really only used in the 'front zone'. Beyond this area, the illuminance level decreases quite significantly, justifying the neglect of the inter-voxel light transmission. This assumption allows a considerable simplification of the global calculation, avoiding the development of a metamodel for a complete building, which is almost impossible because of the too numerous possible configurations of voxels. Thus, in practice, the global *DF* of a modular building is evaluated from the visible envelope of each of its components (here the voxels of which at least one face is in contact with the

outside), then aggregated into an 'average performance' that best promotes the natural lighting of the building, considering any interior voxel as blind.

4.5. Structure and estimation of occluding masks

A solution generated by EcoGen2 is composed of multiple stacked or connected voxels, of the same dimensions, potentially presenting tilted faces and variable degrees of adjacency. Its masks are a priori arbitrary, coming from the built environment and from the self-shadowing of this solution. To each face of the building envelope is attached a list of sensors. A mask structure, *DF_mask*, is associated to each sensor C: it represents an angular discretization (azimuth γ, solar height β) in Moxels of size taille *M* x *M* of the half-sphere of sky visible from the sensor (Figure 4). The sky masking rate is proportional to the solid angle occulted, and is calculated by projecting the contributions of all occulting objects present in the visibility area. By extension to the scale of a window, the calculation of the 'equivalent mask' is obtained by going through all the sensors of this window, and merging (in the Boolean sense) their masks within a *DF_global_mask*: an acceptable approximation at this level of accuracy of calculations.

Moxels play a double role: they measure the occultation of the sky at a point (γ, β) of the discretized angular space [0, γ_{max}] x [0, β_{max}], and they allow to store a depth information of the occluders (Figure 4). In the C++ code, the effective structure is as follows:

```
struct DF_mask
{
// Mox = 0: no occlusion
// Mox > 0: stores the distance to the nearest occluding of the sensor
uchar *Mox[γmax / M + 1][ βmax / M + 1];
};
```

4.6. Transformation of a global mask DF_mask into a valid rectangular mask (d_i, l_i, h_i)

A first difficulty consisted in transforming an occultation mask of arbitrary shape (*DF_global_mask*) into a centred rectangular equivalent with adjustment of the three parameters (d_i, l_i, h_i) in their domain of validity (D), to be able to use the reference polynomial DF_{2014}. The trick was to start again from the luminance calculations to reason about equivalent rectangular masks from the point of view of the loss of sky luminance (the only objective data) in the zone of vision of a sensor or an opening.

Secondly, the tilt angle Σ (Figure 5) of the vertical facades, which was not taken into account before, had to be integrated into the new model. Because, if the orientation of the building does not matter on the calculation of *DF*, it is not the same for the tilt. Rather than redoing tedious calculations, we have shown, as also suggested by (Li, Lau, and Lam 2005), that it is sufficient to evaluate the additional sky luminance received when $\Sigma < 90°$. The consideration of the inclination is done by adding a corrective factor calculated on the luminance curve of the diffuse sky, invariant with the azimuth. It follows an acceptable approximation for low inclinations ($\Sigma > 70°$): $DF(\Sigma) = DF.\frac{L(\Sigma)}{L(90)}$. Note that our model does not handle facades facing the ground ($\Sigma > 90°$).

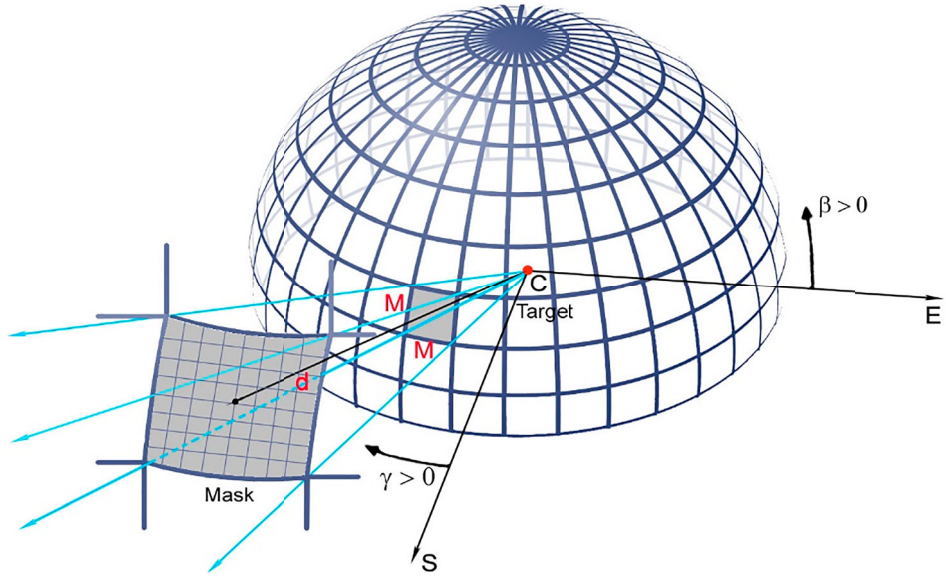

Figure 4. Projection of occultants into the hemispheric Moxels space of a C target/sensor.

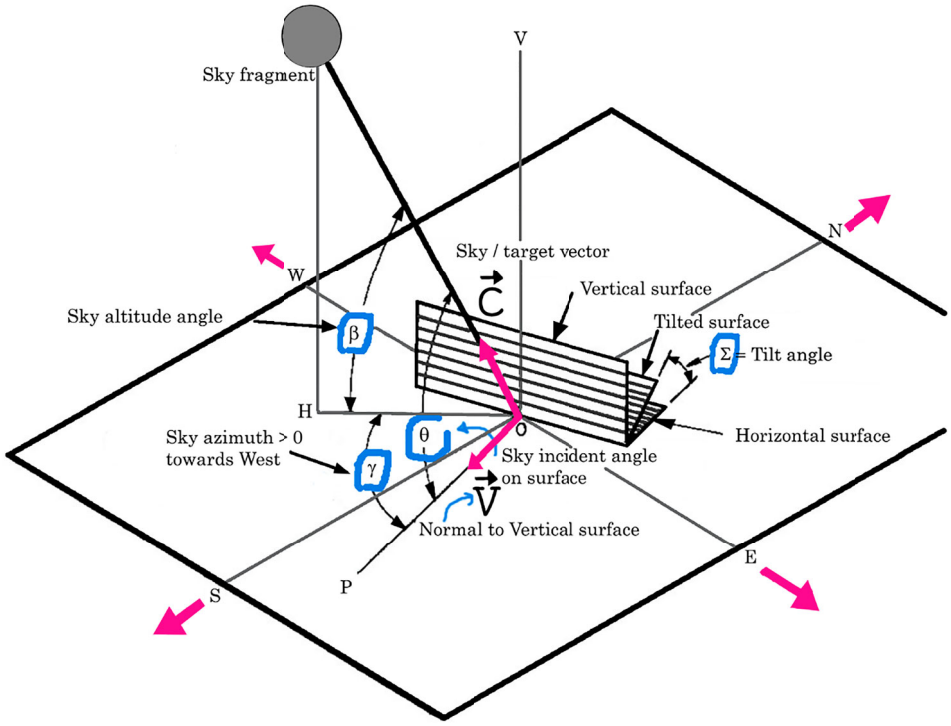

Figure 5. Parameters of the diffuse sky / face interaction.

In (CIE. 'Natural daylight' 1955), the 'CIE overcast luminance' as a function of the sky altitude angle β (Figure 5) is expressed as: $L(\beta) = \frac{L_z}{3}(1 + 2\,sin\beta)$ with $L = 4094$ cd/m^2. The total luminance over the angular height domain [0, β] is therefore calculated as follows:.

$$L[0,\ \beta] = \int_0^{\beta} L(x)\,dx = \frac{L_z}{3}[\beta + 2(1 - \cos\beta)] \qquad \text{(eq.Q)}$$

Another formulation is more useful for estimating the luminance loss due to local masking of a Moxel, i.e. over an interval β:

$$L[\beta,\ \beta + M] = \int_{\beta}^{\beta+M} L(x)\,dx = \frac{L_z}{3} \times [2(\cos\beta - \cos(\beta + M)) + M] \qquad \text{(eq.R)}$$

For efficiency, these $L[\beta,\ \beta{+}M]$ values are precomputed for all useful (β, M) pairs and then stored in the *M_lumin vector* [ ].

Now, the calculation of the parameters (d_i, l_i, h_i) of the mask i of a vertical or skyward sloping face is done via the following steps. First, (eq.R) allows us to evaluate precisely the luminance lost for each Moxel occulted in a *DF_global_mask* relative to an opening. Since azimuth is not involved in the expression of luminance, we can group the terms for the same angle β along an azimuthal path of the *DF_global_mask*, in order to be able to obtain a related rectangular region of dimensions ($D\gamma$, $D\beta$).

We evaluate $D\beta$ (eq.S) by inverting the luminance accumulation function L_{cum} pre-stored in the vector *M_lumin*[ ], through the reciprocal vector *inv_M_lumin*[ ]. In addition, we take into account β*_correct*, a corrective factor for the tilt Σ of the face, allowing us to always bring the angle $D\beta$ to 90° (for a correct use of the polynomial DF_{2014}):

$$D\beta = inv\_M\_lumin[min(L_{cum},\ 9746)] * \beta\_correct[\Sigma] \qquad \text{(eq.S)}$$

Where 9746 is the maximum cumulative luminance for a given azimuth, and β*_correct*$[\Sigma] = 90 / (180 - \Sigma)$.

$D\gamma$ is finally adjusted to obtain the closest and most compact mask to the ground (to avoid out-of-domain mask variables). If there are several choices, the one that provides the most compact (square) mask is taken, to get as far away from the boundary values as possible.

Thus, locally, we find for each opening an admissible mask (rectangular, centred, of optimized size $D\gamma$ x $D\beta$) equivalent to the luminance loss of the diffuse sky.

Then, d_i is obtained by cumulative averaging for each occluded Moxel of the d values associated with the *DF_global_mask* positions (Figure 4). The calculation (eq.T) of l_i and h_i from the angular approximation ($D\gamma$, $D\beta$) is then immediate:

$$l_i = 2d_i.\,tan(D\gamma/2.M)\ ,\ h_i = d_i.\,tan(D\beta.M) \qquad \text{(eq.T)}$$

Finally, if at least one of the parameters (d'_i, l'_i, h'_i) obtained after homothetic realignment (section 4.2)

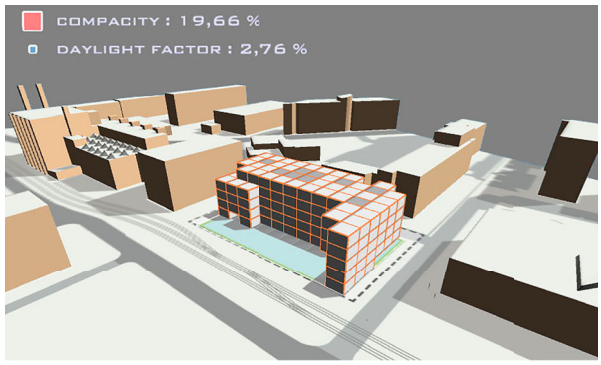

Figure 6. A 5-storey solution (from the Pareto front) within a built-up area, optimizing daylight factor and compactness in EcoGen2.1 (voxel dimensions: L = 5.4 m, W = 5.1 m, H = 3.4 m; grey voxels represent blind rooms, white voxels are luminous ones).

is outside the domain of admissible values (D), it is brought back in by finding an equivalent mask $(\widehat{d_i}, \widehat{d_j}, \widehat{d_k})$ in terms of luminance loss, which is used as input to the DF_{2014} polynomial. As usual, this operation is easily accelerated by a precalculation of the possible valid substitutions.

5. Conclusion

The main objective of this research was to provide, in the early design phase, a realtime evaluation of the daylight factor for a building composed of aggregated modules of the same size per storey, ranging from a dozen to several hundred, in a potentially dense built environment, with many local or distant sky masking effects (figure 6). We have shown that, if the designer knows the type of environment, the centred aperture ratios, the inclinations of the facades and the set of masks shading the different facades, the hybrid metamodel presented in this paper allows to estimate with sufficient accuracy in the sketch phase the daylighting potential within such an assembly of cuboid modules, without resorting to complicated and time-consuming calculations.

Numerous simplifications lead to obtain it, and the main objective of our work was only to obtain an interactive calculation tool, usable for many evaluations in generative design of buildings coupling several performances (light, thermal, shape, structure, …), as within the EcoGen2 software, support of our tests.

We have also contributed to effectively overcome the limits of a previous statistical model with weaknesses (fixed parameters, too restricted domains of variables). The generalization – normally not very fruitful – has been made possible here by returning to physical modeling, and by taking into account quasi-similitude properties.

At last, we have provided architects with totally CPU-based models and computation tools, leaving the GPU power for other high demanding computations in BS. Moreover, in 3D scenes without shading devices or interaction between buildings on a site, there is no advantage to use the GPU for daylight calculations (Marsh and Stravoravdis 2017; Jones and Reinhart 2017). These points appear to be important when it comes to compute in real-time several performances, without mobilizing the full GPU power for a single calculation, which could be detrimental to an entire programme. It is often a question of a balance between CPU and GPU, even though nowadays common computers easily have several of these units. Consequently, our research can be highly beneficial for generative design calculations in the early design phase of a modular project by leaving computation space and time devoted to GPU.

6. Discussion

However, we must emphasize that such a metamodel, even validated by two statistical analyses, cannot in itself be a holistic approach.

We do not claim that the metamodeling of *DF* via the building envelope should systematically replace a more complete and precise modeling of the interior daylighting. It is simply very relevant for the interactive and relatively precise evaluation in the sketch phase of the impact of key technical choices on energy efficiency or interior lighting comfort. This is why it is so useful in generative design, which frequently requires tens of thousands of solution evaluations in a relatively short time.

Obviously, our paper only deals with the simplified case of an assembly of more or less deformable modules. We are far from being able to extend the method and the algorithms to buildings of any shape and construction mode. For reasons of design of experiments and simulation time, metamodeling assumes a parametric description of the building with few variables. Even in this case, the nature of its shape can have a significant influence on the accuracy of the calculations. For example, as also pointed out in (Marsh and Stravoravdis 2017), statistical *DF* metamodeling is less suitable for rooms with very high average surface reflectances and a geometry where one internal dimension is 25% smaller than the other two, or that the only windows are placed on the smaller surface wall.

In addition, the extension to other light metrics than DF (sDA, ASE, UDI), with a similar approach in generative design, is still possible; but the pseudo-affinity is specific to this DF model.

Finally, we experienced a difficulty in daylight metrics optimization of modular buildings, already highlighted in

(Peters et al. 2019), a paper which presents the results of a generative design study to explore alternative geometries for the modular tower building typology. Because a genetic algorithm is responsible for jointly optimizing light penetration (sDA and ASE), cross-ventilation and a panel of viewpoints, this results in mosaic-like volume distributions of voids and solids. Then in order to avoid or limit this kind of fragmentation, one possible solution is to define a range of admissible threshold for *DF* values.

Acknowledgements

The author would like to thank L.E. Mavromatidis for providing his DF_{2014} model and the whole DIALux database used to build it.

Disclosure statement

No potential conflict of interest was reported by the author(s).

References

Ahmad, Danny Asim, Anil Kumar, Om Prakash, and Ankish Aman. 2020. "Daylight availability assessment and the application of energy
simulation software – A literature review." *Materials Science for Energy Technologies* 3 (2020): 679–689. KeAi.

Ayoub, M. 2020. "A review on machine learning algorithms to predict daylighting inside buildings." *Solar Energy* 202: 249–275.

Bollinger, K., M. Grohmann, and O. Tessmann. 2010. "Structured becoming evolutionary processes in design engineering." *The New Structuralism: Design, Engineering and Architectural Technologies. John Wiley & Sons, Ltd*, 80 (4): 34–39.

Box, G., and D. Behnken. 1960. "Some new three level designs for the study of quantitative variables." *Technometrics* 2: 455e75.

Catalina, T., V. Iordache, and B. Caracaleanu. 2013. "Multiple regression model for fast prediction of the heating energy demand." *Energy & Building* 2013 (57): 302e12.

Catalina, T., J. Virgone, and E. Blanco. 2008. "Development and validation of regression models to predict monthly heating demand for residential buildings." *Energy and Buildings* 2008 (40): 1825e43.

Cheung, H. D., and T. M. Chung. 2005. "Calculation of the vertical daylight factor on window facades in a dense urban environment." *Architect Sci Rev* 48 (1): 81e92.

CIE. "Natural daylight". 1955. Official recommendation, Compte Rendu CIE 13, Session 2, Part 3.2.

Crisp, V. H. C., and P. J. Littlefair. 1984. "Average daylight factor prediction." Proceedings CIBS National Lighting Conference, University of Cambridge.

Darmon, I. 2018. "Voxel computational morphogenesis in urban context: proposition and analysis of rules-based generative algorithms considering solar access". MS Design by Data. https://www.researchgate.net/publication/329738763.

De Luca, F., M. Kiil, R. Simson, J. Kurnitski, and R. Murula. 2019. ""Evaluating Daylight Factor Standard through Climate Based Daylight Simulations and Overheating Regulations in Estonia"." Proceedings of the 16th IBPSA Conference, Roma, Italy.

DIALux software. https://www.DIALux.com/.

Dogan, T., and Y. Park. 2017. "A New Framework for Residential Daylight Performance Evaluation".

Garcia, S. 2017. "Classifications of shape grammars." *Design Computing and Cognition* 16: 229–248.

Goupy, J. 2017. *Introduction aux plans d'expériences*. 5ième édition. Paris: Dunod.

Granadeiro, V., J. P. Duarte, J. R. Correia, et al. 2013. "Building envelope shape design in early stages of the design process: integrating architectural design systems and energy simulation." *Automation in Construction* 32: 196–209.

Guan, L. 2020. "An Investigation of Alternative Daylight Metrics". PhD of the Institute for Environmental Design and Engineering University College London.

Hong, T., Z. Wang, X. Luo, and W. Zhang. 2020. "State-of-the-art on research and applications of machine learning in the building life cycle." *Energy and Buildings* 212: 1–40.

Igawa, N., Y. Koga, T. Matsuzawa, and H. Nakamura. 2004. "Models of sky radiance distribution and sky luminance distribution." *Solar Energy* 77: 137e57.

Janjai, S., and P. Plaon. 2011. "Estimation of sky luminance in the tropics using artificial neural networks: modeling and performance comparison with the CIE model"." *Applied Energy* 88: 840–847.

Jones, N. L., and C. F. Reinhart. 2014. "Irradiance caching for global illumination calculation on graphics hardware." 2014 ASHRAE/IBPSA-USA, Building Simulation Conference, Atlanta, GA, *September 10-12*, pp. 111-120.

Jones, N. L., and C. F. Reinhart. 2014. "Physically based global illumination calculation using graphics hardware." *Proceedings of eSim 2014: The Canadian Conference on Building Simulation*, pp. 474-487.

Jones, N. L., and C. F. Reinhart. 2015. "Fast daylight coefficient calculation using graphics hardware." Proc. of BS2015: 14th Conference of International Building Performance Simulation Association, Hyderabad, India.

Jones, N. L., and C. F. Reinhart. 2016. ""Real-Time Visual Comfort Feedback for architectural Design"." PLEA 2016 Los Angeles – 32nd International Conference on Passive and Low Energy Architecture. *Cities, Buildings, People: Towards Regenerative Environments*.

Jones, N. L., and C. F. Reinhart. 2017. ""Speedup Potential of Climate-Based Daylight Modelling on GPUs"." Proceedings of the 15th IBPSA Conference, San Francisco, CA, USA.

Katsanou, Varvara N., Minas C. Alexiadis, and Dimitris P. Labridis. 2019. "An ANN-based model for the prediction of internal lighting conditions and user actions in non-residential buildings." *Journal of Building Performance Simulation* 12 (5): 700–718. doi:10.1080/19401493.2019.1610067.

Kazanasmaz, T., M. Gunaydin, and S. Binol. 2009. "Artificial Neural Networks to Predict Daylight Illuminance in Office Buildings." *Building and Environment* 44 (8): 1751–1757.

Le-Thanh, L., H. Nguyen-Thi-Viet, J. Lee, and H. Nguyen-Xuan. 2022. "Nguyen-Xuan. "Machine learning-based real-time daylight analysis in buildings"." *Journal of Building Engineering* 52: 42–61. doi:10.1016/j.jobe.2022.104374.

Li, D. H. W., N. T. C. Chau, and K. K. W. Wan. 2013. "Predicting daylight illuminance and solar irradiance on vertical surfaces based on classified standard skies." *Energy* 53: 252e8.

Li, D. H. W., C. C. S. Lau, and J. C. Lam. 2005. "Predicting daylight illuminance on inclined surfaces using sky luminance data." *Energy* 30 (9): 1649e85.

Li, D. H., S. Lou, A. Ghaffarianhoseini, K. A. Alshaibani, and J. C. Lam. 2017. "A review of calculating procedures on daylight factor based metrics under various CIE Standard Skies and obstructed environments." *Building and Environment* 112: 29–44.

Lin, C.-H., and Y.-S. Tsay. 2021. "A metamodel based on intermediary features for daylight performance prediction of façade design." *Building and Environment* 206. doi.org/10.1016/j.buildenv.2021.108371.

Lorenz, K. C.-L., M. Packianather, A. B. Spaeth, and C. Bleil De Souza. 2018. "Artificial neural network-based modelling for daylight evaluations." Symposium on Simulation for Architecture & Urban Design.

Loutfi, H., A. Bernatchou, Y. Raoui, and R. Tadili. 2017. "Learning Processes to Predict the Hourly Global, Direct, and Diffuse Solar Irradiance from Daily Global Radiation with Artificial Neural Networks." *International Journal of Photoenergy*, 1–13.

Marsault, X., and F. Torres. 2019. "An interactive and generative eco-design tool for architects in the sketch phase." IOP's Journal of Physics: Conference Series Vol. 1343, november 2019. https://iopscience.iop.org/issue/1742-6596/1343/1.

Marsh, A., and S. Stravoravdis. 2017. "Towards Dynamic Real-Time Daylight Simulation". PLEA'17, Design to Thrive, Edinburgh.

Mavromatidis, L. E., X. Marsault, and H. Lequay. 2014. ""Daylight factor estimation at an early design stage to reduce buildings' energy consumption due to artificial lighting: a numerical approach based on Doehlert and Box–Behnken designs." *Energy, ELSEVIER* 65: 488–502. doi:10.1016/j.energy.2013.12.028.

Mebarki, C., E. Djakab, A. M. Mokhtari, Y. Amrane, and L. Derradji. 2021. "Improvement of Daylight Factor Model for Window Size Optimization and Energy Efficient Building Envelope Design." *Journal of Daylighting* 8: 204–221. doi:10.15627/jd.2021.17.

The MOOVABAT project. 2017–2020. https://www.er2i.eu/fr/moovabat-le-batiment-technologique-intelligent/.

Nabil, A., and J. Mardaljevic. 2006. "Useful daylight illuminances: a replacement for daylight factors." *Energy and Buildings* 38: 905–913.

Naeem, M., and M. Wilson. 2007. "A study of the application of the BRE Average Daylight Factor formula to rooms with window areas below the working plane." 2nd PALENC Conference and 28th AIVC Conference on Building Low Energy Cooling and Advanced Ventilation Technologies in the 21st Century, Crete island, Greece.

Nault, E. 2016. *Solar potential in early neighborhood design - A decision-support workflow based on predictive models*. Lausanne: PhD N°7058, EPFL.

Nourkojouri, H., N. S. Shafavi, M. Tahsildoost, and Z. S. Zomorodian. 2021. "Development of a Machine-Learning Framework for Overall Daylight and Visual Comfort Assessment in Early Design Stages." *Journal of Daylighting* 8: 270–283. doi.org/10.15627/jd.2021.21.

Parker, S., J. Bigler, A. Dietrich, H. Friedrich, J. Hoberock, D. Luebke, D. McAllister, et al. 2010. "OptiX: A general purpose ray tracing engine." *ACM Transactions on Graphics – Proceedings of ACM SIGGRAPH* 29 (4): 1–13.

Perez, R., R. Seals, and J. Michalsky. 1993. "All-weather model for sky luminance distribution preliminary configuration and validation." *Solar Energy* 1993 (50): 235e45.

Peters, T., J. Wolf, B. Peters, and T. Kesik. 2019. "Generative Design Approaches to Daylight in MURBs." Proceedings of the 16th IBPSA Conference, Roma, Italy.

Radziszewski, K., and M. Waczynska. 2018. "Machine learning algorithm-based tool and digital framework for substituting daylight simulations in early-stage architectural design evaluation". Symposium on Simulation for Architecture & Urban Design.

Robert, Shannon. 1979. "Applied optics and optical engineering". Elsevier editor, Vol. 7:p. 45.

Safdie, M. 1961. "A three-dimensional modular building system". Thesis, University of Montreal, Canada.

Si, W., X. Pan, H. Ogai, K. Hirai, N. Yamauchi, and T. Li. 2014. "Illumination Modeling Method for Office Lighting Control by Using RBFNN." *IEICE Transactions on Information and Systems* E97.D (12): 3192–3200.

SpaceMaker software. https://www.spacemakerai.com.

Walger da Fonseca, R., and F. O. Ruttkay Pereira. 2021. "Metamodeling of the Energy Consumption of Buildings with Daylight Harvesting – Application of Artificial Neural Networks Sensitive to Orientation." *Journal of Daylighting* 8: 255–269. doi:10.15627/jd.2021.20.

Wienold, J. 2009. "Dynamic daylight glare evaluation." Eleventh International IBPSA Conference: Building Simulation. pp 944–951.

Woop, S., J. Schmittler, and P. Slusallek. 2005. "RPU: A programmable ray processing unit for realtime ray tracing." *ACM Transactions on Graphics - Proceedings of ACM SIGGRAPH* 24 (3): 434–444.

Xiu, D., G. E. Karniadakis, and D. Xiu. 2002. "The Wiener-Askey polynomial chaos for stochastic differential equations." *Siam Journal. on Scientific Computing* 24: 619–644. (electronic).

Zhou, S., and D. Liu. 2015. "Prediction of Daylighting and Energy Performance Using Artificial Neural Network and Support Vector Machine"." *Am. J. Civ. Eng. Archit* 3 (3A): 1–8.